ACS APPLIED MATERIALS & INTERFACES

Research Article

www.acsami.org

Metal–Organic Frameworks Constructed from D-Camphor Acid: Bifunctional Properties Related to Luminescence Sensing and Liquid-Phase Separation

Lili Wen,*[,†] Xiaoyue Xu,[†] Kangle Lv,[‡] Yumei Huang,[†] Xiaofang Zheng,[†] Li Zhou,[†] Renqiang Sun,[†] and Dongfeng Li*[,†]

[†]Key Laboratory of Pesticide & Chemical Biology of Ministry of Education, College of Chemistry, Central China Normal University, Wuhan, 430079, P. R. China

[‡]Key Laboratory of Catalysis and Materials Science of the State Ethnic Affairs Commission & Ministry of Education, South-Central University for Nationalities, Wuhan 430074, P. R. China

Supporting Information

ABSTRACT: Three metal–organic frameworks (MOFs) $[M_2(D\text{-cam})_2(bimb)_2]_n \cdot 3.5nH_2O$ (M = Mn for **1**, Co for **2**) and $[Cd_8(D\text{-cam})_8(bimb)_4]_n$ (**3**) (D-H_2cam = D-camphor acid, bimb = 4,4′-bis(1-imidazolyl)biphenyl), solvothermally synthesized, exhibit structural diversity. The charming aspect of these frameworks is that compound **3** is the very first MOF-based sensor for quantitatively detecting three different types of analytes (metal ions, aromatic molecules, and pesticides). And also, both compounds **2** and **3** show rapid uptake and ready regeneration for methyl orange (MO) and can selectively bind MO over methylene blue (MB) with high MO/MB separation ratio.

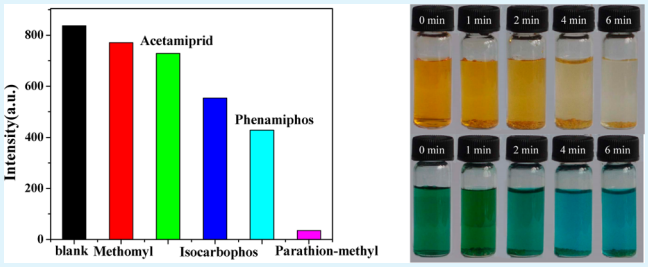

KEYWORDS: *metal–organic frameworks, luminescence quenching, quantitative detecting, dyes separation*

INTRODUCTION

Metal–organic frameworks (MOFs), constructed from metal ions or clusters and organic ligands, represent a class of organic–inorganic hybrid crystalline materials with adjustable pore structures and large surface areas, which have demonstrated great potential applications in energy- and environment-related fields, most notably hydrogen and greenhouse gases storage.[1−6] Recently, there is an increasing trend in using luminescence MOFs to probe guest species and thus develop multifunctional MOFs that combine luminescence and other promising applications, such as magnetism and biomedicine.[7−11] However, only very limited MOFs for simultaneously detecting diverse kinds of analytes were investigated;[12,13] quite few luminescent MOF sensors have been discovered that are capable of quantitative detection, until now.[14−16] In addition, due to their high porosities,[17,18] relatively heterogeneous surface,[19] as well as potentially strong electrostatic interactions with the guest species,[20,21] MOFs are of high interest in liquid-phase adsorption and separation,[22−26] which is very scarce compared to the abundant research in the gas phase to date. The selectivity and recyclability, particularly the stability of these MOFs, need to be enhanced. Considering the many dyes that are toxic and even carcinogenic, a significant issue is the removal of dyes from contaminated water.[27]

In our effort, which is aimed toward multifunctional MOFs, flexible D-camphor acid (D-H_2cam),[28−34] rigid 4,4′-bis(1-imidazolyl)biphenyl (bimb), and transition-metal centers (Mn^{2+}/Co^{2+}/Cd^{2+}) were selected to construct new structures with potential applications in luminescence sensing and liquid-phase separation based on the following considerations: (1) the binding between D-H_2cam and metal centers not only adds flexibility and diversity in the structures but also alters the electronic structures and surface functionalities of the MOFs, which may direct their specific recognition for guest substrates through host–guest interactions; (2) rigid ligand bimb with aromatic π rings may effectively favor intraligand interactions and promote luminescent character. Herein, we present three MOFs, namely, $[M_2(D\text{-cam})_2(bimb)_2]_n \cdot 3.5nH_2O$ (M = Mn for **1**, Co for **2**) and $[Cd_8(D\text{-cam})_8(bimb)_4]_n$ (**3**), which exhibit structural diversity. The charming aspect of these frameworks is that compound **3** is the very first MOF-based sensor for quantitative detection of three different types of analytes (metal ions, aromatic molecules, and pesticides). And also, both compounds **2** and **3** show rapid uptake and ready regeneration for methyl orange (MO) and can selectively bind MO over methylene blue (MB) with high MO/MB separation ratio.

EXPERIMENTAL SECTION

Materials and Measurements. All chemicals were obtained from commercial source and used without further purification. Elemental

Received: January 9, 2015
Accepted: February 5, 2015
Published: February 5, 2015

DOI: 10.1021/acsami.5b00160
ACS Appl. Mater. Interfaces 2015, 7, 4449−4455

analyses (C, H, and N) were determined on a PerkinElmer 240 elemental analyzer. IR spectra were obtained on a Bruker Vector 22 spectrophotometer with KBr discs in the 4000−400 cm^{-1} region. Thermogravimetric analysis (TGA) measurements were conducted on a TA-SDT 2960 at a heating rate of 10 °C min^{-1} in nitrogen atmosphere. Powder X-ray diffraction (PXRD) data were obtained on a Siemens D5005 diffractometer with Cu Kα (λ = 1.540 56 Å) radiation over the 2θ range of 5−50°. Luminescent spectra were recorded with a Hitachi 850 fluorescence spectrophotometer. The photoluminescence lifetime was measured on Edinburgh instruments FLS920 fluorescence spectrometer. UV−vis spectra were collected on a TU-1900 double-beam spectrophotometer.

*Syntheses of $[M_2$(D-cam)$_2$(bimb)$_2]_n \cdot 3.5nH_2O$ (M = Mn for **1**, Co for **2**).* A mixture of $MnCl_2 \cdot 4H_2O$ (19.7 mg, 0.10 mmol), D-H_2cam (20.0 mg, 0.10 mmol), bimb (14.3 mg, 0.05 mmol) in a mixed *N*,*N*-dimethylacetamide and water (DMA/H_2O, 1 mL/2 mL) solvent was placed in a parr Teflon-lined stainless steel vessel (25 mL) and heated at 130 °C for 3 d, then slowly cooled to room temperature. Colorless crystals of **1** were collected in 11% yield based on manganese. Anal. Calcd for $C_{112}H_{112}Mn_4N_{16}O_{23}$: C, 59.26; H, 4.97; N, 9.87%; found: C, 59.21; H, 5.07; N, 9.83%. IR spectrum (cm^{-1}): 3358m, 2886w, 2360w, 1589s, 1518m, 1395m, 1371m, 1356m, 1309w, 1262w, 1122w, 1066m, 1023w, 961w, 930w, 816m, 794w, 753m. Compound **2** was synthesized by a solvothermal procedure similar to that described for **1** except using $Co(NO_3)_2 \cdot 6H_2O$ instead of $MnCl_2 \cdot 4H_2O$ and heated at 120 °C for 2 d. Violet crystals of **2** were obtained in 73% yield based on cobalt. Anal. Calcd for $C_{112}H_{112}Co_4N_{16}O_{23}$: C, 58.85; H, 4.94; N, 9.80%; found: C, 58.89; H, 5.07; N, 9.82%. IR spectrum (cm^{-1}): 2977s, 2781s, 2440m, 1702m, 1588m, 1518m, 1471w, 1385s, 1311w, 1125w, 1065w, 1024w, 963w, 826w, 853w.

*Synthesis of $[Cd_8$(D-cam)$_8$(bimb)$_4]_n$ (**3**).* Compound **3** was prepared by using a similar procedure except with $Cd(NO_3)_2 \cdot 6H_2O$ (30.8 mg, 0.1 mmol) replacing $MnCl_2 \cdot 4H_2O$ in a solvent mixture of DMA/CH_3OH (1.5 mL/1.5 mL). Colorless crystals of **3** were obtained in 62% yield based on cadmium. Anal. Calcd for $C_{152}H_{168}Cd_8N_{16}O_{32}$: C, 50.29; H, 4.66; N, 6.17%; found: C, 50.32; H, 4.76; N, 6.22%. IR spectrum (cm^{-1}): 3127w, 2963m, 2881w, 1631w, 1520s, 1459w, 1397s, 1365m, 1312w, 1262m, 1171w, 1127w, 1067m, 962w, 938w, 819m, 759w.

X-ray Crystallography. The X-ray diffraction intensity data for compounds **1** and **2** were collected on a Bruker Smart Apex DUO CCD diffractometer with Mo Kα radiation at 298 K. The diffraction data for compound **3** was measured on a Bruker D8 QUEST PHOTON 100 CMOS detector with TRIUMPH curved crystal monochromator for Mo Kα radiation at 173 K. Data reductions and absorption corrections were, respectively, performed with the SAINT[35] and SADABS[36] software packages. The structure was solved by direct methods and refined anisotropically on F^2 by the full-matrix least-squares technique using the SHELXL-97.[37] For **3**: the guest solvent molecules were highly disordered, which could not be modeled as discrete atomic sites. In this structure, free solvent molecules were removed using the SQUEEZE routine of PLATON,[38,39] and the structure was then refined again using the data generated. Crystallographic data and structure refinement information for **1**−**3** are listed in Supporting Information, Table S1.

RESULTS AND DISCUSSION

Description of the Crystal Structures. *$[M_2$(D-cam)$_2$(bimb)$_2]_n \cdot 3.5nH_2O$ (M = Mn for **1**, Co for **2**).* The unit cell parameter measurements from selected crystals reveal that compounds **1** and **2** are isomorphous; therefore, only the structure of compound **1** was analyzed in detail. Compound **1** crystallizes in the orthorhombic crystal system of the $P2_12_12$ chiral space group. There are two independent Mn^{2+} atoms, two D-cam^{2-} anions, two bimb bridges, and two free aqua molecules, as well as three one-half guest water molecules in the asymmetric unit. As illustrated in Figure 1a, each Mn^{2+} atom is six-coordinated with distorted octahedral coordination geometry, composed of four oxygen atoms from two individual D-cam^{2-} moieties with both carboxylate groups in μ^1-η^1:η^1 coordination mode and two nitrogen donors from two separate bimb ligands. The Mn−O distances fall in the range of 2.202(2)−2.262(2) Å, and the Mn−N bonds lengths are from 2.195(3) to 2.223(3) Å, both of which are close to those reported for mangnese(II) complexes with D-cam^{2-} and N-donor auxiliary ligands.[40] The single two-dimensional (2D) layer for compound **1** is accomplished by D-cam^{2-} and bimb interlinking the metal centers (Supporting Information, Figure S1a). Apparently, the Mn(II) centers were viewed as four-connectors bridging two D-cam^{2-} moieties and two bimb linkers, and thus the topology[41,42] of **1** is a 4-connected **sql** net with its point (Schläfli) symbol of ($4^4 \cdot 6^2$). The interesting feature of **1** is the occurrence of an inclined interpenetrating motif involving two identical single nets, giving a 2-fold interpenetrated 2D → 2D network (Figure 1b and Supporting Information, Figure S1b).

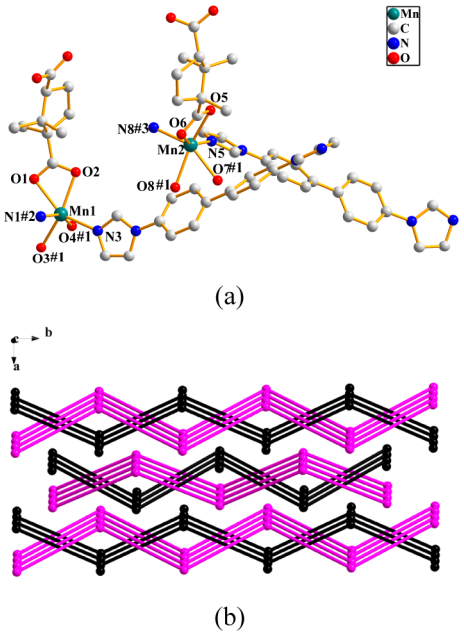

Figure 1. (a) Coordination environment of Mn atom with hydrogen atoms and free water omitted for clarity of **1**. Symmetry codes: No. 1 *x*, *y*, 1 + *z*; No. 2 1.5 − *x*, 0.5 + *y*, 1 − *z*; No. 3 0.5 − *x*, 0.5 + *y*, 2 − *z*. (b) The schematic view of 2-fold interpenetration of **1**.

*$[Cd_8$(D-cam)$_8$(bimb)$_4]_n$ (**3**).* Compound **3** was solved in the chiral space group $P2_1$. There are eight Cd(II) atoms, eight D-cam^{2-} anions, and four neutral bimb bridges in the asymmetric unit. As illustrated in Figure 2a, each Cd^{2+} center also sits in a distorted octahedron sphere, which contains five oxygen atoms from three independent D-cam^{2-} moieties and one bimb nitrogen atom. The Cd−O and Cd−N bond lengths are in the range of 2.150(5)−2.501(17) Å and 2.058(8)−2.406(7) Å, respectively. On the other hand, each D-cam^{2-} anion binds three Cd(II) atoms through two carboxylate groups in μ^1-η^1:η^1 and μ^2-η^2:η^1 coordination fashions, respectively, and each rigid bimb links two Cd(II) ions, thereby resulting in a 2D layer structure for **3** (Supporting Information, Figure S2c). Especially in **3**, each dinuclear cadmium subunit $[Cd_2(COO)_2]$, generated by double carboxylate groups connecting adjacent a pair of independent Cd(II) atoms, is surrounded by another six dimers; therefore, compound **3** adopts a six-connected **hxl** net with Schläfli symbol ($3^6 \cdot 4^6 \cdot 5^3$, Figure 2b).

DOI: 10.1021/acsami.5b00160
ACS Appl. Mater. Interfaces 2015, 7, 4449−4455

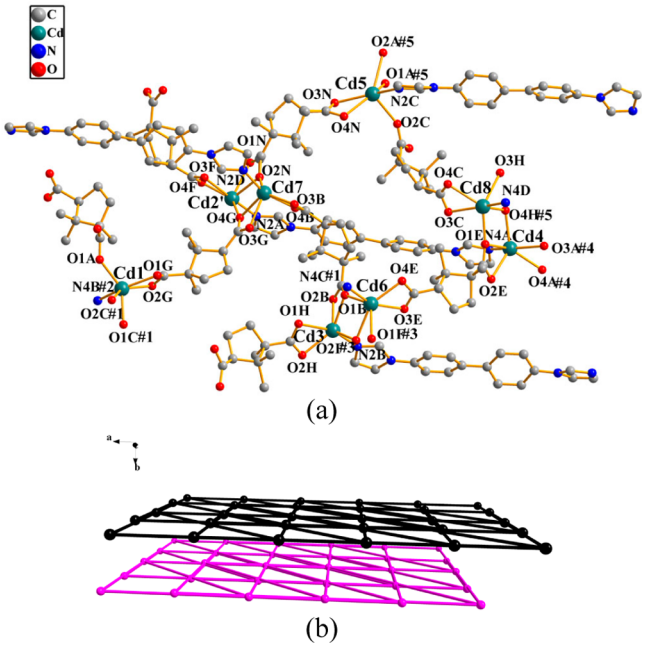

Figure 2. (a) Coordination environment of Cd atom with hydrogen atoms omitted for clarity of **3**. Symmetry codes: No. 1 *x*, *y*, −1 + *z*; No. 2 1 + *x*, *y*, −1 + *z*; No. 3−1 + *x*, *y*, *z*; No. 4 −1 + *x*, *y*, 1 + *z*; No. 5 *x*, *y*, 1 + *z*. (b) The schematic view of 2D layer of **3**.

PXRD of the Complexes. For complexes **2** and **3**, the similarity of simulated PXRD pattern from single-crystal data with that for as-synthesized sample indicating the phase purities (Supporting Information, Figure S2). The PXRD profiles of **2** and **3** underline that the framework retains intact after recycling test for MO removal and immersion in acetone or dimethylformamide (DMF) solution. For compound **1**, the yield was too low to collect enough pure samples for PXRD.

Luminescence Sensing. The solid-state photoluminescence (PL) spectra of as-synthesized **3** and free ligand bimb were investigated upon excitation at 300 nm under ambient temperature. Compound **3** exhibits a strong band at ∼370 nm and an obvious blue-shift compared with the organic linker (λ_{em} = 410 nm), which may arise from the ligand-centered emission (Supporting Information, Figure S4a). The luminescence lifetime of compound **3** is as follows: τ_1 = 1.5032 ns (Supporting Information, Figure S4b). Interestingly, compound **3** in distinct solvent emulsions displays strong guest-dependent luminescence properties, which shows the most significant quenching effect toward acetone, implying that the compound can be considered as a candidate for selective detection of acetone (Figure 3a). It is noticeable that acetone exhibits a wide absorption range from 225 to 325 nm, whereas the excitation spectrum of compound **3** centered at ∼300 nm, which is apparently overlapped by the absorption band of acetone. Therefore, the significant PL quenching effect could be ascribed to the energy transfers between the organic ligand and solvent molecule upon excitation.[43,44] Furthermore, a gradual depression of the PL intensity was observed upon the addition of acetone to the DMF emulsion of **3**, and the PL intensity of **3** centered at 370 nm versus the volume ratio of acetone could well be fitted to first-order exponential decay function, demonstrating that PL quenching of **3** by acetone is diffusion-controlled (Supporting Information, Figure S5).

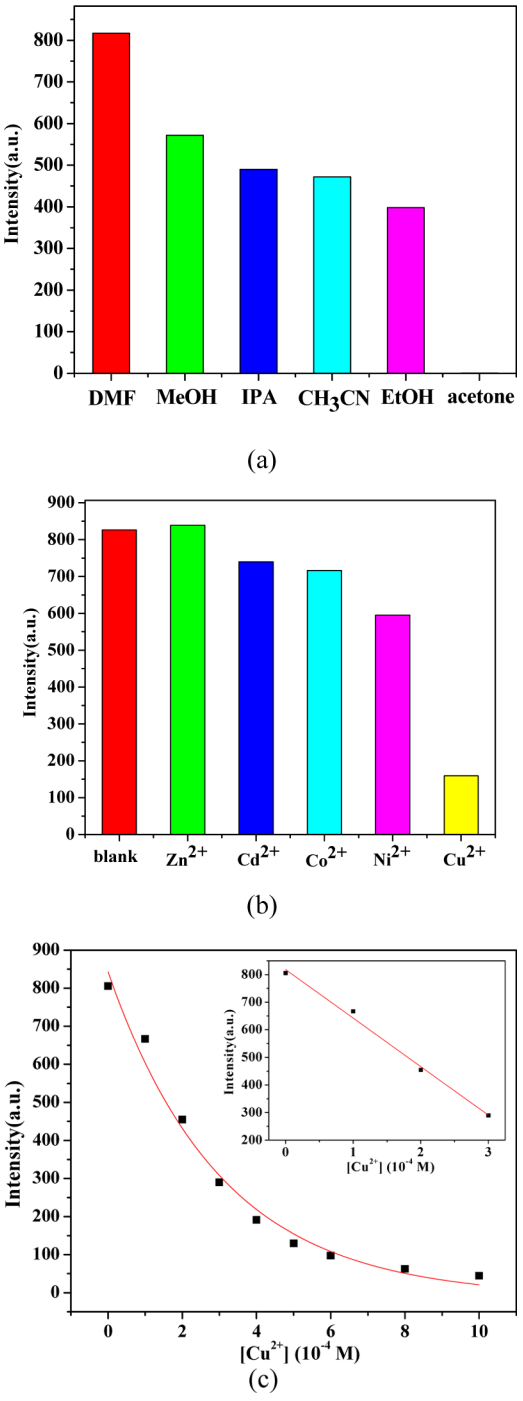

Figure 3. PL intensities of compound **3** introduced to various pure solvents (a) and different metal ions (b) in DMF. (c) The PL intensities of **3** as a function of Cu^{2+} at different concentrations in DMF. (inset) The emission quenching linearity relationship of **3** below 3 × 10^{-4} M (I = −160.552 84c + 802.642 87, R = 0.993 76) excited at 300 nm.

Meanwhile, the potential applications of **3** in sensing metal ions were also examined. The 5 mg as-synthesized **3** was dispersed in 5 mL of DMF individually containing 1.0 × 10^{-2} mol·L^{-1} $M(NO_3)_2$ (M = Co^{2+}, Ni^{2+}, Cu^{2+}, Zn^{2+}, and Cd^{2+}) for the sensing studies. As shown in Figure 3b, the PL intensities of M-incorporated **3** emulsions are heavily metal ion-dependent. Apparently, the introduction of Zn^{2+} has a negligible effect on the PL intensity, while addition of cations Cd^{2+}, Co^{2+}, Ni^{2+}, and

DOI: 10.1021/acsami.5b00160
ACS Appl. Mater. Interfaces 2015, 7, 4449−4455

Cu^{2+} can cause PL quenching in various degrees. In particular, the PL intensity of **3** is dramatically quenched by ~80% upon addition of Cu^{2+}, underlining the bright potential of compound **3** for the sensing of Cu^{2+}, which may be interpreted that the d−d transition of Cu^{2+} wasted the energy of the system.[45−50] To explore sensitivity toward Cu^{2+} in detail, a batch of emulsions of **3** dispersed in DMF solutions containing different amounts of Cu^{2+} were prepared to monitor the emissive response (Supporting Information, Figure S6). Clearly, as shown in Figure 3c, the PL intensity decreases gradually with the increase of the Cu^{2+} concentration, and the inset illustrates that the emission quenching of **3** is linear to $Cu(NO_3)_2$ concentration below 3.0×10^{-4} mol·L^{-1} at 370 nm. The detection limit (LOD) of 5.805×10^{-6} mol·L^{-1} toward Cu^{2+} in DMF suspension for compound **3** is calculated from the equation: LOD = kS_b/m, where k = 3, S_b is the standard deviation of the blank sample, and m is the slope of the calibration graph in the linear range. The investigation of luminescent sensors of Cu^{2+} with high selectivity and sensitivity is remarkably attractive, due to its potential significance in living biological systems.

Rapid and efficient detection of explosives and explosive-like substances is very important to homeland security and environmental safety; therefore, the detecting of nitro-aromatic molecules by MOFs is also an important topic.[51−59] The intensity of the PL in **3** are largely dependent on the aromatics, exhibiting significant quenching behavior in the case of nitrobenzene, which may be related to the electron transfer from the electron-donating MOF to the highly electron-deficient nitrobenzene molecule upon excitation (Figure 4a). To examine sensitivity toward nitrobenzene in more detail, a batch of suspensions of **3** with gradually increasing nitrobenzene content was prepared to monitor the emissive response (Supporting Information, Figure S7a). Supporting Information, Figure S7b shows the emission quenching of **3** is linear to nitrobenzene content below 3.27×10^{-4} mol·L^{-1} at 300 nm. The detection limit toward nitrobenzene in DMF suspension for compound **3** is 6.972×10^{-6} mol·L^{-1}.

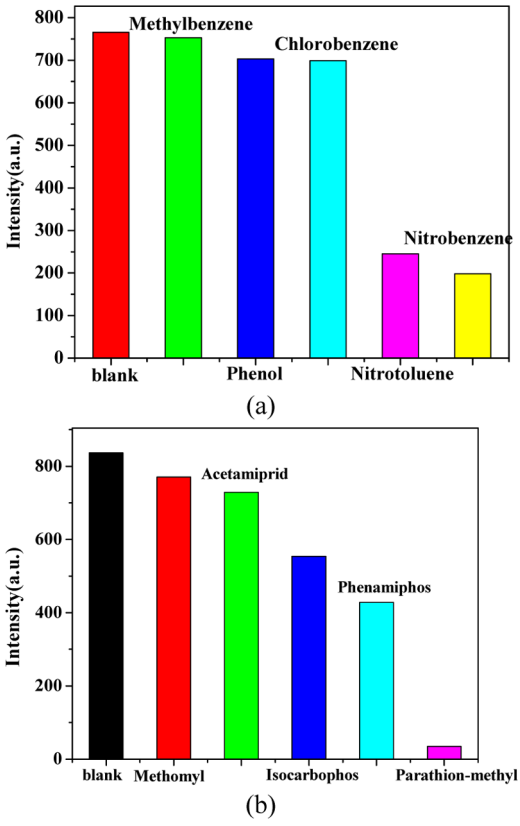

Figure 4. PL intensities of **3** toward selective aromatic molecules with concentration of 6.5×10^{-4} M (a) and relevant pesticides with concentration of 1×10^{-3} M (b) in DMF.

Owing to the high toxicity of pesticides, rapid determination and reliable quantification of a trace level of pesticides for pest control have aroused increasing attention.[60−63] Therefore, inspired by the work to utilize **3** for the sensing nitrobenzene, the potential of complex **3** for the detecting of nitro-containing pesticides was carried out. The effects of 1×10^{-3} mol·L^{-1} relevant pesticides (Supporting Information, Scheme S1) in DMF on the fluorescence response of **3** were recorded. Strikingly, the results indicate that among the different pesticides tested, compound **3** exhibits the most effective detection of parathion-methyl: the PL intensity decreased to 60% at 1×10^{-4} mol·L^{-1}, and complete quenching was received at 1×10^{-3} mol·L^{-1}. The encouraging result reveals **3** could be a promising luminescent probe for nitro-containing pesticide. Furthermore, Supporting Information, Figure S8b shows the emission quenching of **3** linearly correlates with parathion-methyl concentration below 1×10^{-4} mol·L^{-1} at 370 nm, and the detection limit reaches 3.576×10^{-6} mol·L^{-1}. To the best of our knowledge, **3** is the very first MOF-based sensor for quantitatively detecting three different types of analytes (metal ions, aromatic molecules, and pesticides) simultaneously through fluorescence quenching, although limited MOFs for detecting one or two of them were investigated.[64,65]

Liquid-Phase Separation. Methyl orange (MO) and methylene blue (MB) (Supporting Information, Scheme S2) are the most common acidic/anionic and basic/cationic dyes. To study the adsorption ability of compound **2** for dyes, 20 mg of crystals of **2** were dipped into an aqueous solution of MO (20 ppm, 4 mL) at ambient temperature. The MO was completely removed from aqueous solution during 4 min with the yellow MO solution fading rapidly to colorless and the MO concentration almost decreasing to zero. On the contrary, no evident color changes were observed for the blue MB solution during the same process, and the MB concentration in water decreased slightly (from the initial 20 ppm to final 19.8 ppm); therefore, the adsorptive capacity of **2** for MB is negligible (Figure 5a,b). In the case of **3** as an adsorbent, it showed quite similar performance to that of compound **2**, which also can effectively remove MO from water. The yellow MO solution turned rapidly to nearly colorless after 6 min with the MO concentration decreasing to the final 0.21 ppm. But the adsorptive removal of **3** for MB is negligible as the MB concentration hardly changed (from the initial 20 ppm to final 19.9 ppm) during the process (Supporting Information, Figure S9). The regeneration of adsorbent **2** and **3** was achieved by simply soaking the MO-loaded **2** and **3** in a fresh DMF solution for 4 min, mixed well with magnetic stirring under ambient temperature. Remarkably, the colorless DMF solution changed to yellow, accompanying with absorbents **2** and **3** almost returning to the original color (Supporting Information, Figure S10). A recycling test with three consecutive runs was carried out for **2** and **3** to check whether the adsorbent could be reused for subsequent removal (Supporting Information, Figure S11). Specifically, for all three repetitive runs, the adsorptive removal ability of **2** and **3** for MO did not descend, suggesting the

DOI: 10.1021/acsami.5b00160
ACS Appl. Mater. Interfaces 2015, 7, 4449−4455

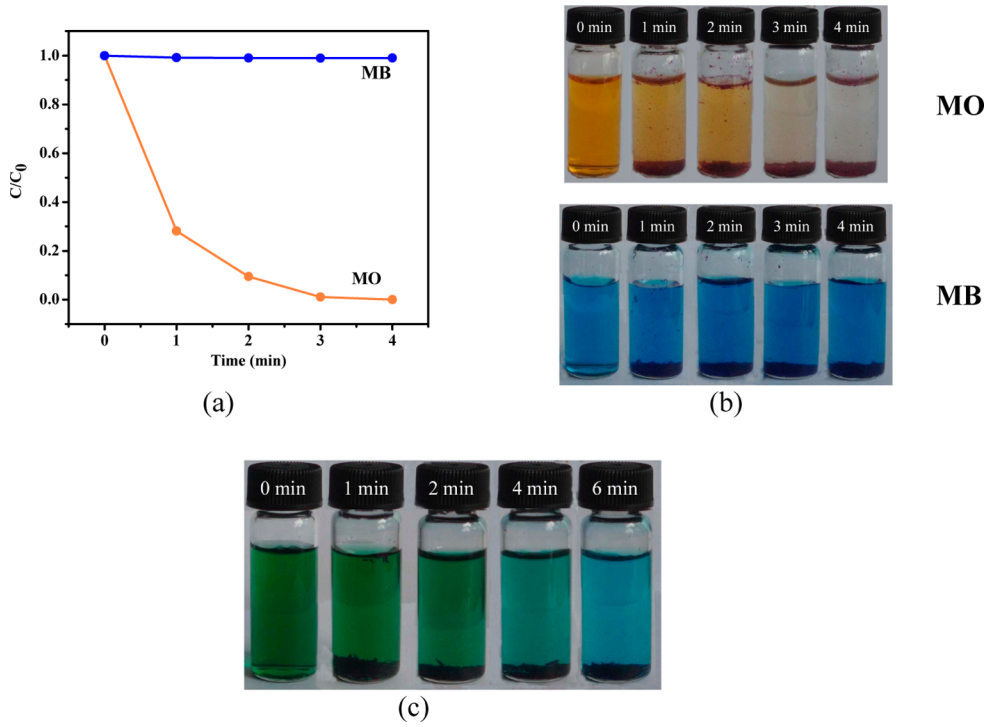

Figure 5. (a) Concentration curves of MO and MB. (b) Photos of enrichment progress over **2** in 4 min. (c) Photos showing the selective adsorption of MO over MB by **2**.

applicability of MOFs in the adsorptive removal of anionic dye from wastewater.

Such strong adsorption toward MO for compounds **2** and **3** inspire us to further study the potential application of these complexes in selective separation MO from an MO−MB mixture. Twenty milligrams of crystals of **2** or **3** were soaked in a mixture of MO (20 ppm) and MB (20 ppm) aqueous solution (4 mL), which quickly changed from green to blue after 6 min (Figure 5c and Supporting Information, Figure S9). According to the equation of working curve for single system monitored by UV−vis spectrometer (Supporting Information, Figure S12), in the presence of adsorbent **2** and **3**, the content of MO in the mixture individually sharply decreases to 1.57 and 2.84 ppm, while the final concentration of MB is 17.64 and 19.58 ppm, respectively. The MO/MB separation ratio for adsorbent **2** and **3** is thus calculated to be 7.81:1 and 40.86:1. Such fast and selective removal of MO over MB in water for compounds **2** and **3** can be mainly attributed to an electrostatic interaction between the metal cation centers (Co^{2+} or Cd^{2+}) with strong positive electric field effect and anionic MO in addition to the $\pi-\pi^*$ interaction between benzene rings of MOF and dyes. The results demonstrate that compounds **2** and **3** exhibit highly selective and recyclable properties in removal of MO dye from contaminated water.

CONCLUSIONS

In summary, we present three MOFs, namely, $[M_2(\text{D-cam})_2(\text{bimb})_2]_n \cdot 3.5nH_2O$ (M = Mn for **1**, Co for **2**) and $[Cd_8(\text{D-cam})_8(\text{bimb})_4]_n$ (**3**), which exhibit structural diversity. The charming aspect of these frameworks is that compound **3** is the very first MOF-based sensor for quantitatively detecting three different types of analytes (metal ions, aromatic molecules, and pesticides). And also, both compounds **2** and **3** show rapid uptake and ready regeneration for the methyl orange (MO) and can selectively bind MO over methylene blue (MB) with high MO/MB separation ratio.

ASSOCIATED CONTENT

Supporting Information

X-ray crystallographic file (CIF), additional crystal figures and molecular structures, fluorescence measurements, tabulated crystallographic data for complexes **1**−**3**, PXRD patterns, TGA data, emission spectra, decay lifetime fitting and fluorescence sensing for complex **3**, dye adsorption and separation for complexes **2** and **3**, recycling test data. This material is available free of charge via the Internet at http://pubs.acs.org.

AUTHOR INFORMATION

Corresponding Authors

*E-mail: wenlili@mail.ccnu.edu.cn. (L. Wen)
*E-mail: dfli@mail.ccnu.edu.cn. Fax: + 86 27 67867232. Phone: +86 27 67862900. (D. Li)

Notes

The authors declare no competing financial interest.

ACKNOWLEDGMENTS

This work was financially supported by the National Nature Science Foundation of China (Nos. 21171062, 21371065, and 21172084), Program for Chenguang Young Scientists of Wuhan (2013070104010020).

REFERENCES

(1) Suh, M. P.; Park, H. J.; Prasad, T. K.; Lim, D.-W. Hydrogen Storage in Metal−Organic Frameworks. *Chem. Rev.* **2012**, *112*, 782−835.
(2) Li, J. R.; Sculley, J.; Zhou, H. C. Metal-Organic Frameworks for Separations. *Chem. Rev.* **2012**, *112*, 869−932.
(3) Yun, R. R.; Lu, Z. Y.; Pan, Y.; You, X. Z.; Bai, J. F. Formation of a Metal−Organic Framework with High Surface Area and Gas Uptake

DOI: 10.1021/acsami.5b00160
ACS Appl. Mater. Interfaces 2015, 7, 4449−4455

by Breaking Edges Off Truncated Cuboctahedral Cages. *Angew. Chem., Int. Ed.* **2013**, *52*, 11282−11285.
(4) Zhao, Y. X.; Seredych, M.; Zhong, Q.; Bandosz, T. J. Superior Performance of Copper Based MOF and Aminated Graphite Oxide Composites as CO_2 Adsorbents at Room Temperature. *ACS Appl. Mater. Interfaces* **2013**, *5*, 4951−4959.
(5) Policicchio, A.; Zhao, Y. X.; Zhong, Q.; Agostino, R. G.; Bandosz, T. J. Cu-BTC/Aminated Graphite Oxide Composites as High-Efficiency CO_2 Capture Media. *ACS Appl. Mater. Interfaces* **2014**, *6*, 101−108.
(6) Wang, C.; Li, L. J.; Tang, S. F.; Zhao, X. B. Enhanced Uptake and Selectivity of CO_2 Adsorption in a Hydrostable Metal−Organic Frameworks *via* Incorporating Methylol and Methyl Groups. *ACS Appl. Mater. Interfaces* **2014**, *6*, 16932−16940.
(7) Cui, Y. J.; Yue, Y. F.; Qian, G. D.; Chen, B. L. Luminescent Functional Metal−Organic Frameworks. *Chem. Rev.* **2012**, *112*, 1126−1162.
(8) Kreno, L. E.; Leong, K.; Farha, O. K.; Allendorf, M.; Van Duyne, R. P.; Hupp, J. T. Metal−Organic Framework Materials as Chemical Sensors. *Chem. Rev.* **2012**, *112*, 1105−1125.
(9) McKinlay, A. C.; Morris, R. E.; Horcajada, P.; Férey, G.; Gref, R.; Couvreur, P.; Serre, C. BioMOFs: Metal−Organic Frameworks for Biological and Medical Applications. *Angew. Chem., Int. Ed.* **2010**, *49*, 6260−6266.
(10) Taylor-Pashow, K. M. L.; Rocca, J. D.; Xie, Z.; Tran, S.; Lin, W. Postsynthetic Modifications of Iron-Carboxylate Nanoscale Metal−Organic Frameworks for Imaging and Drug Delivery. *J. Am. Chem. Soc.* **2009**, *131*, 14261−14263.
(11) Hatakeyama, W.; Sanchez, T. J.; Rowe, M. D.; Serkova, N. J.; Liberatore, M. W.; Boyes, S. G. Synthesis of Gadolinium Nanoscale Metal-Organic Framework with Hydrotropes: Manipulation of Particle Size and Magnetic Resonance Imaging Capability. *ACS Appl. Mater. Interfaces* **2011**, *3*, 1502−1510.
(12) Liu, G. L.; Qin, Y. J.; Jing, L.; Wei, G. Y.; Li, H. Two Novel MOF-74 Analogs Exhibiting Unique Luminescent Selectivity. *Chem. Commun.* **2013**, *49*, 1699−1701.
(13) Zheng, X. F.; Zhou, L.; Huang, Y. M.; Wang, C. G.; Duan, J. G.; Wen, L. L.; Tian, Z. F.; Li, D. F. A Series of Metal−Organic Frameworks Based on 5-(4-Pyridyl)-Isophthalic Acid: Selective Sorption and Fluorescence Sensing. *J. Mater. Chem. A* **2014**, *2*, 12413−12422.
(14) Ma, D. X.; Li, B. Y.; Zhou, X. J.; Zhou, Q.; Liu, K.; Zeng, G.; Li, G. H.; Shi, Z.; Feng, S. H. A Dual Functional MOF as a Luminescent Sensor for Quantitatively Detecting the Concentration of Nitrobenzene and Temperature. *Chem. Commun.* **2013**, *49*, 8964−8966.
(15) Wang, J. H.; Li, M.; Li, D. A Dynamic, Luminescent and Entangled MOF as a Qualitative Sensor for Volatile Organic Solvents and a Quantitative Monitor for Acetonitrile Vapour. *Chem. Sci.* **2013**, *4*, 1793−1801.
(16) Xu, X. Y.; Yan, B. Eu(III)-Functionalized MIL-124 as Fluorescent Probe for Highly Selectively Sensing Ions and Organic Small Molecules Especially for Fe(III) and Fe(II). *ACS Appl. Mater. Interfaces* **2014**, DOI: 10.1021/am5070409.
(17) Haque, E.; Lee, J. E.; Jang, I. T.; Hwang, Y. K.; Chang, J.-S.; Jegal, J.; Jhung, S. H. Adsorptive Removal of Methyl Orange from Aqueous Solution with Metal-Organic Frameworks, Porous Chromium-Benzenedicarboxylates. *J. Hazard. Mater.* **2010**, *181*, 535−542.
(18) Huang, X. X.; Qiu, L. G.; Zhang, W.; Yuan, Y. P.; Jiang, X.; Xie, A. J.; Shen, Y. H.; Zhu, J. F. Hierarchically Mesostructured MIL-101 Metal−Organic Frameworks: Supramolecular Template-Directed Synthesis and Accelerated Adsorption Kinetics for Dye Removal. *CrystEngComm* **2012**, *14*, 1613−1617.
(19) Huo, S. H.; Yan, X. P. Metal−Organic Framework MIL-100(Fe) for the Adsorption of Malachite Green from Aqueous Solution. *J. Mater. Chem.* **2012**, *22*, 7449−7455.
(20) Haque, E.; Jun, J. W.; Jhung, S. H. Adsorptive Removal of Methyl Orange and Methylene Blue from Aqueous Solution with a Metal-Organic Framework Material, Iron Terephthalate (MOF-235). *J. Hazard. Mater.* **2011**, *185*, 507−511.
(21) Tong, M. M.; Liu, D. H.; Yang, Q. Y.; Devautour-Vinot, S.; Maurin, G.; Zhong, C. L. Influence of Framework Metal Ions on the Dye Capture Behavior of MIL-100 (Fe, Cr) MOF Type Solids. *J. Mater. Chem. A* **2013**, *1*, 8534−8537.
(22) Sun, L. B.; Xing, H. Z.; Liang, Z. Q.; Yu, J. H.; Xu, R. R. A 4 + 4 Strategy for Synthesis of Zeolitic Metal−Qrganic Frameworks: an Indium-MOF with SOD Topology as a Light-Harvesting Antenna. *Chem. Commun.* **2013**, *49*, 11155−11157.
(23) Jiang, H. L.; Tatsu, Y.; Lu, Z. H.; Xu, Q. Non-, Micro-, and Mesoporous Metal−Organic Framework Isomers: Reversible Transformation, Fluorescence Sensing, and Large Molecule Separation. *J. Am. Chem. Soc.* **2010**, *132*, 5586−5587.
(24) Tan, Y. X.; He, Y. P.; Wang, M.; Zhang, J. A Water-Stable Zeolite-Like Metal−Organic Framework for Selective Separation of Organic Dyes. *RSC Adv.* **2014**, *4*, 1480−1483.
(25) Zou, C.; Zhang, Z. J.; Xu, X.; Gong, Q. H.; Li, J.; Wu, C. D. A Multifunctional Organic−Inorganic Hybrid Structure Based on Mn^{III}−Porphyrin and Polyoxometalate as a Highly Effective Dye Scavenger and Heterogenous Catalyst. *J. Am. Chem. Soc.* **2012**, *134*, 87−90.
(26) Jin, L. N.; Liu, Q.; Yang, Y.; Fu, H. G.; Sun, W. Y. Large-Scale Preparation of Indium-Based Infinite Coordination Polymer Hierarchical Nanostructures and Their Good Capability for Water Treatment. *J. Colloid Interface Sci.* **2014**, *426*, 1−8.
(27) Tong, M.; Zhao, D.; Xie, L.; Liu, D.; Yang, Q.; Zhong, C. Treatment of Waste Water Using Metal-Organic Frameworks. *Prog. Chem.* **2012**, *24*, 1646−1655.
(28) Zhang, J.; Chen, S. M.; Valle, H.; Wong, M.; Austria, C.; Cruz, M.; Bu, X. H. Manganese and Magnesium Homochiral Materials: Decoration of Honeycomb Channels with Homochiral Chains. *J. Am. Chem. Soc.* **2007**, *129*, 14168−14169.
(29) Zhang, J.; Bu, X. H. Temperature Dependent Charge Distribution in Three-Dimensional Cadmium Camphorates. *Chem. Commun.* **2008**, 444−446.
(30) Zhang, J.; Yao, Y. G.; Bu, X. H. Comparative Study of Homochiral and Racemic Chiral Metal-Organic Frameworks Built from Camphoric Acid. *Chem. Mater.* **2007**, *19*, 5083−5089.
(31) Chen, N.; Li, M. X.; Yang, P.; He, X.; Shao, M.; Zhu, S. R. Chiral Coordination Polymers with SHG-Active and Luminescence: An Unusual Homochiral 3D MOF Constructed from Achiral Components. *Cryst. Growth Des.* **2013**, *13*, 2650−2660.
(32) Blake, K. M.; Gandolfo, C. M.; Uebler, J. W.; LaDuca, R. L. Diverse Topologies in Chiral Divalent Metal Camphorate Coordination Polymers Containing 4,4′-Dipyridylamine. *Cryst. Growth Des.* **2012**, *12*, 5125−5137.
(33) Yang, P.; He, X.; Li, M. X.; Ye, Q.; Ge, J. Z.; Wang, Z. X.; Zhu, S. R.; Shao, M.; Cai, H. L. The First Homochiral Coordination Polymer with Temperature-Independent Piezoelectric and Dielectric Properties. *J. Mater. Chem.* **2012**, *22*, 2398−2400.
(34) Liang, X. Q.; Li, D. P.; Zhou, X. H.; Sui, Y.; Li, Y. Z.; Zuo, J. L.; You, X. Z. Metal−Organic Coordination Polymers Generated from Chiral Camphoric acid and Flexible Ligands with Different Spacer Lengths: Syntheses, Structures and Properties. *Cryst. Growth Des* **2009**, *9*, 4872−4883.
(35) *SAINT,* version 6.2; Bruker AXS, Inc.: Madison, WI, 2001.
(36) Sheldrick, G. M. *SADABS;* University of Göttingen: Göttingen, Germany, 1997.
(37) Sheldrick, G. M. *SHELXTL,* version 6.10; Bruker Analytical X-ray Systems: Madison, WI, 2001.
(38) Vandersluis, P.; Spek, A. L. BYPASS: an Effective Method for the Refinement of Crystal Structures Containing Disordered Solvent Regions. *Acta Crystallogr.* **1990**, *A46*, 194−201.
(39) Spek, A. L. Single-Crystal Structure Validation with the Program PLATON. *J. Appl. Crystallogr.* **2003**, *36*, 7−13.
(40) Dang, D. B.; An, B.; Bai, Y.; Zheng, G. S.; Niu, J. Y. Three-Dimensional Homochiral Manganese−Lanthanide Frameworks Based on Chiral Camphorates with Multi-Coordination Modes. *Chem.Commun.* **2013**, *49*, 2243−2245.

DOI: 10.1021/acsami.5b00160
ACS Appl. Mater. Interfaces 2015, 7, 4449−4455

(41) Blatov, V. A. *TOPOS,* A Program Package for Multipurpose Crystallochemical Analysis; Samara State University: Samara, Russia, 2004.
(42) Blatov, V. A.; Proserpio, D. M. *Acta Crystallogr. Sect. A: Found. Crystallogr.* **2009**, *63*, 329−442.
(43) Meng, X.; Song, X. Z.; Song, S. Y.; Yang, G. C.; Zhu, M.; Hao, Z. M.; Zhao, S. N.; Zhang, H. J. A Multifunctional Proton-Conducting and Sensing Pillar-Layer Framework Based on [24-MC-6] Heterometallic Crown Clusters. *Chem. Commun.* **2013**, *49*, 8483−8485.
(44) Hao, Z. M.; Yang, G. C.; Song, X. Z.; Zhu, M.; Meng, X.; Zhao, S. N.; Song, S. Y.; Zhang, H. J. A Europium(III) Based Metal−Organic Framework: Bifunctional Properties Related to Sensing and Electronic Conductivity. *J. Mater. Chem. A* **2014**, *2*, 237−244.
(45) Zhao, B.; Chen, X. Y.; Chen, Z.; Shi, W.; Cheng, P.; Yan, S. P.; Liao, D. Z. A Porous 3D Heterometal-Organic Framework Containing Both Lanthanide and High-Spin Fe(II) Ions. *Chem. Commun.* **2009**, 3113−3115.
(46) Bünzli, J. C. G.; Piguet, C. Taking Advantage of Luminescent Lanthanide Ions. *Chem. Soc. Rev.* **2005**, *34*, 1048−1077.
(47) Edder, C.; Piguet, C.; Bünzli, J. C. G.; Hopfgartner, G. High-Spin Iron(II) as a Semitransparent Partner for Tuning Europium(III) Luminescence in Heterodimetallic d−f Complexes. *Chem.—Eur. J.* **2001**, *7*, 3014−3024.
(48) Chen, B. L.; Wang, L. B.; Xiao, Y. Q.; Fronczek, F. R.; Xue, M.; Cui, Y. J.; Qian, G. D. A Luminescent Metal−Organic Framework with Lewis Basic Pyridyl Sites for the Sensing of Metal Ions. *Angew. Chem., Int. Ed.* **2009**, *48*, 500−503.
(49) Thibon, A.; Pierre, V. C. A Highly Selective Luminescent Sensor for the Time-Gated Detection of Potassium. *J. Am. Chem. Soc.* **2009**, *131*, 434−435.
(50) Lu, W. G.; Jiang, L.; Feng, X. L.; Lu, T. B. Three-Dimensional Lanthanide Anionic Metal−Organic Frameworks with Tunable Luminescent Properties Induced by Cation Exchange. *Inorg. Chem.* **2009**, *48*, 6997−6999.
(51) Lan, A. J.; Li, K. H.; Wu, H. H.; Olson, D. H.; Emge, T. J.; Ki, W.; Hong, M. C.; Li, J. A Luminescent Microporous Metal−Organic Framework for the Fast and Reversible Detection of High Explosives. *Angew. Chem., Int. Ed.* **2009**, *48*, 2334−2338.
(52) Pramanik, S.; Zheng, C.; Zhang, X.; Emge, T. J.; Li, J. New Microporous Metal-Organic Framework Demonstrating Unique Selectivity for Detection of High Explosives and Aromatic Compounds. *J. Am. Chem. Soc.* **2011**, *133*, 4153−4155.
(53) Xue, Y. S.; He, Y. B.; Zhou, L.; Chen, F. J.; Xu, Y.; Du, H. B.; You, X. Z.; Chen, B. L. A Photoluminescent Microporous Metal Organic Anionic Framework for Nitroaromatic Explosive Sensing. *J. Mater. Chem. A* **2013**, *1*, 4525−4530.
(54) Xu, H.; Liu, F.; Cui, Y. J.; Chen, B. L.; Qian, G. D. A Luminescent Nanoscale Metal−Organic Framework for Sensing of Nitroaromatic Explosives. *Chem. Commun.* **2011**, *47*, 3153−3155.
(55) Zhang, C. Y.; Che, Y. K.; Zhang, Z. X.; Yang, X. M.; Zang, L. Fluorescent Nanoscale Zinc(II)-Carboxylate Coordination Polymers for Explosive Sensing. *Chem. Commun.* **2011**, *47*, 2336−2338.
(56) Gong, Y. N.; Jiang, L.; Lu, T. B. A Highly Stable Dynamic Fluorescent Metal−Organic Framework for Selective Sensing of Nitroaromatic Explosives. *Chem. Commun.* **2013**, *49*, 11113−11115.
(57) Kim, T. K.; Lee, J. H.; Moon, D.; Moon, H. R. Luminescent Li-Based Metal−Organic Framework Tailored for the Selective Detection of Explosive Nitroaromatic Compounds: Direct Observation of Interaction Sites. *Inorg. Chem.* **2013**, *52*, 589−595.
(58) Li, L. N.; Zhang, S. Q.; Xu, L. J.; Han, L.; Chen, Z. N.; Luo, J. H. An Intensely Luminescent Metal-Organic Framework Based on a Highly Light-Harvesting Dyclo-Metalated Iridium(III) Unit Showing Effective Detection of Explosives. *Inorg. Chem.* **2013**, *52*, 12323−12325.
(59) Zhang, S. R.; Du, D. Y.; Qin, J. S.; Bao, S. J.; Li, S. L.; He, W. W.; Lan, Y. Q.; Shen, P.; Su, Z. M. A Fluorescent Sensor for Highly Selective Detection of Nitroaromatic Explosives Based on a 2D, Extremely Stable, Metal−Organic Framework. *Chem.—Eur. J.* **2014**, *20*, 3589−3594.
(60) Zhang, W. Y.; Asiri, A. M.; Liu, D. L.; Du, D.; Lin, Y. H. Nanomaterial-Based Biosensors for Environmental and Biological Monitoring of Organophosphorus Pesticides and Nerve Agents. *TrAC, Trends Anal. Chem.* **2014**, *54*, 1−10.
(61) Li, H. B.; Qu, F. G. Synthesis of CdTe Quantum Dots in Sol-Gel-Derived Composite Silica Spheres Coated with Calix[4]arene as Luminescent Probes for Pesticides. *Chem. Mater.* **2007**, *19*, 4148−4154.
(62) Wen, L. L.; Zhou, L.; Zhang, B. G.; Meng, X. G.; Qu, H.; Li, D. F. Multifunctional Amino-Decorated Metal−Organic Frameworks: Nonlinear-Optic, Ferroelectric, Fluorescence Sensing and Photocatalytic Properties. *J. Mater. Chem.* **2012**, *22*, 22603−22609.
(63) Wang, F.; Zhao, J. B.; Gong, J. M.; Wen, L. L.; Zhou, L.; Li, D. F. New Multifunctional Porous Materials Based on Inorganic−Organic Hybrid Single-Walled Carbon Nanotubes: Gas Storage and High-Sensitive Detection of Pesticides. *Chem.—Eur. J.* **2012**, *18*, 11804−11810.
(64) Cui, J. H.; Lu, Z. Z.; Li, Y. Z.; Guo, Z. J.; Zheng, H. G. A Microporous Metal−Organic Framework with FeS_2 Topology Based on $[Zn_6(\mu_6\text{-}O)]$ Cluster for Reversible Sensing of Small Molecules. *Chem. Commun.* **2012**, *48*, 7967−7969.
(65) Lu, Z. Z.; Zhang, R.; Li, Y. Z.; Guo, Z. J.; Zheng, H. G. Solvatochromic Behavior of a Nanotubular Metal-Organic Framework for Sensing Small Molecules. *J. Am. Chem. Soc.* **2011**, *133*, 4172−4174.

DOI: 10.1021/acsami.5b00160
ACS Appl. Mater. Interfaces 2015, 7, 4449−4455